Proglacial lakes substantially modulate the surface mass balance of deglacial ice sheets

Lianne Sijbrandij[1], Uta Krebs-Kanzow[1], Paul Gierz[1], Gregor Knorr[1], Lu Niu[1], Shan Xu[1], and Gerrit Lohmann[1,2]

[1]Alfred Wegener Institute Helmholtz Centre for Polar und Marine Research (AWI), Am Alten Hafen 26, 27568 Bremerhaven, Germany
[2]MARUM-Center for Marine Environmental Sciences, University of Bremen, Leobener Straße, 28359 Bremen, Germany

Correspondence: Uta Krebs-Kanzow (uta.krebs-kanzow@awi.de)

Abstract. During the last deglaciation, large proglacial lakes formed along the margins of retreating continental ice sheets. While proglacial lakes are commonly regarded as promoting ice-sheet retreat through dynamic interactions with the ice margin, their influence on the climate may instead have acted to stabilize retreat. Sustained by meltwater inflow and iceberg calving, these lakes likely remained cold throughout summer and may have modified the regional climate, potentially reducing ice-sheet melt. ~~While proglacial lakes are commonly regarded as promoting ice-sheet retreat through dynamic interactions with the ice margin, their climatic influence may instead act to stabilize retreat.~~ Here, we quantify this atmospheric feedback for the Laurentide and Fennoscandian ice sheets using an atmospheric model in combination with an ice-sheet surface mass balance scheme in simulations representative of the Allerød (∼13 thousand years before present), which was a period during which large proglacial lakes formed at the margins of both the North American and European ice sheets. We show that cold proglacial lakes reduce summer air temperatures over a broad surrounding region, while decreasing precipitation and increasing the snow-to-rain ratio. These effects are enhanced when lake temperatures are constrained below 4 °C to represent continued cooling by meltwater inflow and iceberg calving. In our simulation, total melt decreases by 18 % and 27 % for the Laurentide and Fennoscandian ice sheets, respectively, and by 23 % and 35 % with additional lake cooling. These sensitivity experiments demonstrate that cold proglacial lakes can partially offset the positive dynamic feedbacks associated with deglacial lake formation, highlighting an important stabilizing climate feedback during ice-sheet retreat.

1 Introduction

Towards the end of the last glacial period, large proglacial lakes (PLs) have evolved along the margins of the retreating northern hemisphere ice sheets which covered areas comparable to today's Baltic Sea. Prominent examples are the Baltic Ice Lake south of the Fennoscandian Ice Sheet (FIS) covering about 300,000 km^2 (Patton et al., 2017), and Lake Agassiz south of the Laurentide Ice Sheet (LIS) possibly covering more than 150,000 km^2 (Teller et al., 2002). The diversity of drainage and runoff routing histories from the North American ice sheets and the Great Lakes into the Arctic, subpolar Atlantic, and the Gulf of Mexico may have played a pivotal role in the complex northern hemispheric climate evolution (Fisher, 2020). In recent years several studies (Quiquet et al., 2021; Hinck et al., 2022; Austermann et al., 2022; Scherrenberg et al., 2024; Hu and

Haseloff, 2025) have highlighted the dynamic response of the Laurentide Ice Sheets to proglacial lakes as a positive feedback for deglacial ice mass loss. Ice-contact proglacial lakes affect the dynamics of the neighbouring ice sheet through various mechanisms which have an overall negative effect on the mass balance. In particular, PLs may influence location and velocity of ice streams (e.g. Stokes and Clark (2004); Demidov et al. (2006)) and trigger dramatic mass loss similar to the marine ice sheet instability (MISI (Weertman, 1974; Schoof, 2007)). For the deglaciation of the Laurentide Ice Sheet, the coupled simulations with an Earth system model of intermediate complexity from Quiquet et al. (2021) suggest that proglacial lakes cause additional mass loss of 3000 Gt per year, which however likely overestimates the dynamic effect.

In comparison to marine terminating glaciers, lake terminating glaciers are more prone to form floating ice shelves and mass changes will be primarily controlled by the balance between dynamical response and surface mass balance (SMB = snowfall - melt + refreezing), as basal melt is reduced due to lower water temperatures, lower density contrasts and weaker density driven circulation (Truffer and Motyka, 2016). While the positive SMB-elevation feedback seems to play a great role in accelerating the deglaciation (supplement, Scherrenberg et al. (2024)), the climate response and corresponding SMB change due to the existence of proglacial lakes has not been represented or discussed in any of the above studies. ~~Even though sensitivity studies have pointed out~~ Sensitivity studies have shown that proglacial lakes can lead to colder summer temperatures over adjacent ice sheets (Hostetler et al., 2000; Krinner et al., 2004; Mangerud et al., 2004; Carrivick and Tweed, 2013), ~~likely causing~~ potentially resulting in a substantial increase in ~~SMB, we are not aware of any studies providing estimates for~~ surface mass balance (SMB). However, to our knowledge, no studies have quantified the resulting negative SMB feedback for the Laurentide Ice Sheet. More generally, a comparison of the opposing feedbacks of accelerated dynamic mass loss and increased SMB is difficult. For Eurasian Ice Sheets some studies provide a comparison of SMB estimates with and without proglacial lakes (Peyaud et al., 2007; Colleoni et al., 2009; Krinner et al., 2004). These studies indicate that proglacial lakes may reduce surface melt by approximately 25 % and thus increase SMB substantially. None of these studies consider the SMB response during a deglaciation (i.e. in a period of elevated ablation) and all SMB estimates were either obtained by empirical downscaling schemes (temperature-index methods, not capturing regional difference due to radiation or albedo) or diagnosed by climate models of insufficient resolution (absolute values are not reliable). Furthermore Hostetler et al. (2000) pointed out that ice-contact proglacial lakes enhance regional cooling more than other lakes because melting ice in the lakes consumes additional heat: the melting of 1000 Gt of calving icebergs and floating ice shelves would be sufficient to adiabatically cool 8100 km^3 of water by 10 K - an aspect which might shape the chronology of a deglaciation that is not represented in any of the existent SMB estimates.

Therefore we here aim to separately quantify the SMB response to the presence of proglacial lakes for both the Laurentide and Fennoscandian Ice Sheets in three equilibrated simulations with (i) no proglacial lakes, (ii) with proglacial lakes at the margins of both ice sheets and (iii) with the proglacial lakes being additionally cooled to remain below 4 °C in order to mimic the effect of heat loss due to the presence of melting ice in the lakes. We conduct these sensitivity experiments under otherwise identical deglacial boundary conditions representative of the Aller~~ø~~ød, the second part of the B~~ø~~ølling- Aller~~ø~~ød interstadial (13.9-12.9 ka, thousand years before present), a warm excursion from the last deglaciation associated with a strengthening of the Atlantic Meridional Overturning Circulation and increasing Northern Hemisphere summer insolation. During this interval,

rapid retreat of the Laurentide and Fennoscandian ice sheets led to the widespread development of large proglacial lakes. We use an atmospheric general circulation model with a novel modification for the cold proglacial lakes, in combination with a physics based energy balance model as a downscaling interface to resolve the narrow ablation zone of the ice sheets (section 2.) and investigate climate and SMB response to prescribed proglacial lakes (sections 3.1. and 3.2). This approach also allows us to investigate regional differences in the air temperature-melt relation, to identify limitations of empirical temperature-index methods (section 3.3).

2 Materials and Methods

We use the global atmosphere model ECHAM6 (Stevens et al., 2013; Giorgetta et al., 2013) at a horizontal resolution of approximately 1.85° × 1.85° (T63) with 47 vertical levels coupled with the land surface model JSBACH3.2 (Reick et al., 2013) for dynamic vegetation. A thermodynamic lake scheme is part of ECHAM6 where lakes are represented as a single 10m deep, homogenous layer with the capability to form lake ice but without dynamics. The three experiments apply prescribed boundary conditions and forcings representative of the Allerød interstadial at 13 ka. These conditions include 13 ka orography and land ice cover according to the GLAC1D reconstruction (Tarasov et al., 2012) (Fig. S1 in the Supplement), constant 13 ka orbital parameters (Berger, 1978) and atmospheric greenhouse gas concentration (Köhler et al., 2017). However, ocean surface conditions and land sea mask, not available for 13 ka, were taken from a 15 ka simulation with the global coupled climate model AWI-ESM2 (Sidorenko et al., 2019) that has been integrated for 1000 years under constant 15ka boundary conditions, orbital parameters and atmospheric greenhouse gas concentration. Monthly means of sea surface temperature and sea ice concentration averaged over the last 100 model years have been used to drive the model. This somewhat hybrid setup appears to be appropriate for a first sensitivity study which primarily considers response to changes in the land surface, but would not be suitable for a realistic simulation of the deglaciation. In any event, the drivers of the ~~Allerød~~ Allerød interstadial are poorly understood and the millennial-scale variations during a fundamental climate transition are almost impossible to reproduce in coupled climate simulations- a more consistent model set-up would not necessarily be more realistic. Our atmosphere model experiments only differ in the representation of lakes.

Experiment REF13ka Experiment REF13ka is considered the reference simulation. Here, lakes are removed in ice covered regions but otherwise are identical with the present day land surface as in Sidorenko et al. (2019).

Experiment PL13ka: This scenario has implemented a more realistic lake configuration as it includes additional lakes along the margins of the Fennoscandian and Laurentide Ice Sheets (FIS-PL and LIS-PL hereafter). The location of these lakes was identified by the lakeCC tool (Hinck et al., 2020) for the 13ka land surface from the GLAC1D reconstruction. Apart from these additional lakes this experiment is identical with experiment REF13ka. In this experiment all lakes are treated identically with lake temperatures evolving freely according to a mixed layer scheme (Giorgetta et al., 2013).

Experiment PL13ka$_{cold}$: During a deglaciation with dramatic mass loss at the lake-ice interface, proglacial lakes can be assumed to have a cold surface (Hostetler et al., 2000), to be well mixed and to have rarely exceeded 4°C, due to melting of icebergs calving from the adjacent ice sheets and glacial meltwater runoff (Andersen and Borns, 1994; Vincent et al., 2010).

The PL13ka$_{cold}$ scenario uses the same lake configuration as experiment PL13ka, but uses the novel subroutine added to the ECHAM6 source code (Sijbrandij, 2022), which implements that PLs are commonly cold even in summer due to the influence of meltwater from the neighboring ice sheets. The proglacial lakes are distinguished from lakes in REF13ka by an additional mask, which activates a modified lake surface temperature calculation, to the effect that surface temperatures cannot exceed 4 °C. Surface temperatures of all other lakes evolve freely.

All experiments have run for 350 years. We consider the first 250 years as spin-up after which atmosphere and land surface exhibit no noticeable drift in near surface climate and appear to be sufficiently equilibrated. We use the last 100 years to analyze the climate. Finally, we interpolate monthly means of precipitation, near surface temperature, surface downward shortwave and longwave radiation and cloud cover of the analysis period to 5 km resolution and force the surface mass balance model, dEBM (Krebs-Kanzow et al., 2021), to obtain surface mass balance, run-off and accumulation (i.e. snow fall and refreezing). The dEBM is an energy and mass balance scheme, which downscales the monthly forcing from the coarse resolution atmosphere model and implicitly accounts for the diurnal cycle of insolation (Krebs-Kanzow et al., 2018). In a model intercomparison the dEBM demonstrated good agreement with the observed surface mass balance of the present-day Greenland Ice sheet (GrSMBMIP, Fettweis et al. (2020)). In the following we focus on differences between REF13ka and PL13ka$_{cold}$, additional analysis of experiment PL13ka can be found in the Appendix.

3 Results

3.1 Climate response

~~Overall~~**General climate response** ~~Primarily the additional lakes in experiments~~ Introducing lakes in experiment PL13ka ~~and PL13ka$_{cold}$ lead to regionally cooler summers~~adds substantial heat storage capacity that regionally dampens the seasonal cycle relative to experiment REF, yielding cooler, ~~while the effect on the winter season is weak. As per experimental design, the cooling effect is amplified~~ later-onset summers (Fig. 1) but elevated autumn temperatures (not shown). The cooler lake surfaces increase surface air pressure, which suppress advection of humid air and cloud formation. Consequently we observe a drier climate around the lakes with reduced spring and summer precipitation, while autumn precipitation may be enhanced in some locations. Because summer precipitation dominates the seasonal cycle over North America and Europe (Fig. S6 in the Supplement), this reduction translates into lower annual-mean precipitation along the ice-sheet margins (Fig. 2). The additional cooling of the lake surface in experiment PL13ka$_{cold}$ ~~due to the suppression of summer warming. The additional cooling of lake waters is thought~~ further amplifies the effect on summer temperatures and precipitation (Fig. 1 and 2), while suppressing the autumn warming and wetting.

Experiment PL13ka$_{cold}$ is intended to represent the ~~heat loss due to~~ additional heat loss from melting ice shelves and ~~ice bergs~~ icebergs within the lakes. To quantify this effect, we ~~employ~~ use a simple one-dimensional lake model – described in the Supplemental Material – to estimate the ice melt required to ~~achieve~~ produce comparable cooling. ~~The one-dimensional lake model is described in the Supplemental Material.~~ Lake model experiments indicate that ~~200 to 400~~200–400 Gt of ice melt per year would be sufficient to ~~maintain a lake surface area of~~ keep a 100,000 km^2 lake surface below 4 °C year-round for lakes at

the southern margins of the Fennoscandian and Laurentide Ice Sheets, respectively. ~~Thus, experiment~~ Experiment PL13ka$_{cold}$ ~~may be an extreme scenario, but~~ therefore lies at the lower end of what seems realistic, though it could still be ~~realistic in periods of ongoing deglaciation , especially considering proglacial lake-ice~~ plausible during periods of active deglaciation – particularly given proglacial lake–ice sheet instability (PLISI; Quiquet et al. (2021))~~with~~ , which can drive massive ice loss at the lake interface. In the following we consider summer 2m temperatures (June, July, August; JJA) and yearly mean precipitation as the key drivers of surface mass balance and focus on regions around the FIS and LIS. Fig. 1 shows for both regions the distributions of summer near surface temperatures and annual mean precipitation in experiment REF13ka together with respective anomalies for experiments PL13ka and PL13ka$_{cold}$ relative to REF13ka. Above the lake centers summer temperatures are reduced by up to 5 °C and 10 °C in PL13ka and PL13ka$_{cold}$ respectively. In experiment PL13ka parts of the lakes also exhibit positive temperature anomalies, which likely reflects the delayed but longer warm season due to the unconstrained heat uptake and storage of the lakes. On a larger scale temperature gradients in summer between ice sheets and ice free land surface are weakened and shifted away from the ice sheets due to the lakes. Associated with this shift is a displacement in precipitation patterns and reduced precipitation over the lakeward slopes of the ice sheets. These general characteristics are in good agreement with sensitivities found in Colleoni et al. (2009) for the penultimate glaciation. A similar difference in seasonality between experiments with unconstrained and with limited surface warming of PLs is also found in Hostetler et al. (2000). Mean precipitation (summer and winter) and temperature anomalies (summer and winter) on a larger scale are also given in the supplement (Figs S2, S3, S4, S5).

Effect of the proglacial lakes on the Fennoscandian Ice Sheet (FIS-PL). The existence of the FIS-PLs in experiment PL13ka$_{cold}$ reduces summer temperatures significantly over the largest parts of the ice sheet with anomalies lower than -1°C over the grid cells adjacent to the lakes. (Fig. 1)

Interpolated to the 5 km grid and averaged over the Fennoscandian ice sheet JJA 2m temperature exhibits a reduction of 1.21 °C (0.9 °C) for PL13ka$_{cold}$ (PL13ka). The annual mean precipitation over the FIS is reduced by less than 3 % in experiments PL13ka and PL13ka$_{cold}$ but local changes are only significant over the interior (Fig. 2).

Effect of the proglacial lakes on the Laurentide Ice Sheet (LIS-PL). Around the LIS-PLs large scale (>500 km) cooling is visible and 2m temperature anomalies are lower than -1°C over most parts of the ~~Eastern~~ eastern Laurentide Ice Sheet in experiment PL13ka$_{cold}$ (Fig. 1). Similar, yet weaker patterns are found in experiment PL13ka. During the winter months lake surface temperatures are colder than 4 °C in all experiments and lakes are mostly ice covered. In consequence differences in albedo and heat fluxes are small between experiments (not shown) and temperature anomalies are weak and mostly insignificant on a larger scale. Averaged over the entire ice sheet at 5 km resolution summer 2 m temperature anomalies are of the order of -0.9 °C (-0.8 °C) in the PL13ka$_{cold}$ (PL13ka) experiment. In experiment REF13ka the southeastern margins of the ice sheet are zones of high precipitation with intensified precipitation towards the East (Fig. 2). In experiment PL13ka$_{cold}$ the center of the high precipitation region has moved away from the ice sheet and annual precipitation averaged over the ice sheet is reduced by

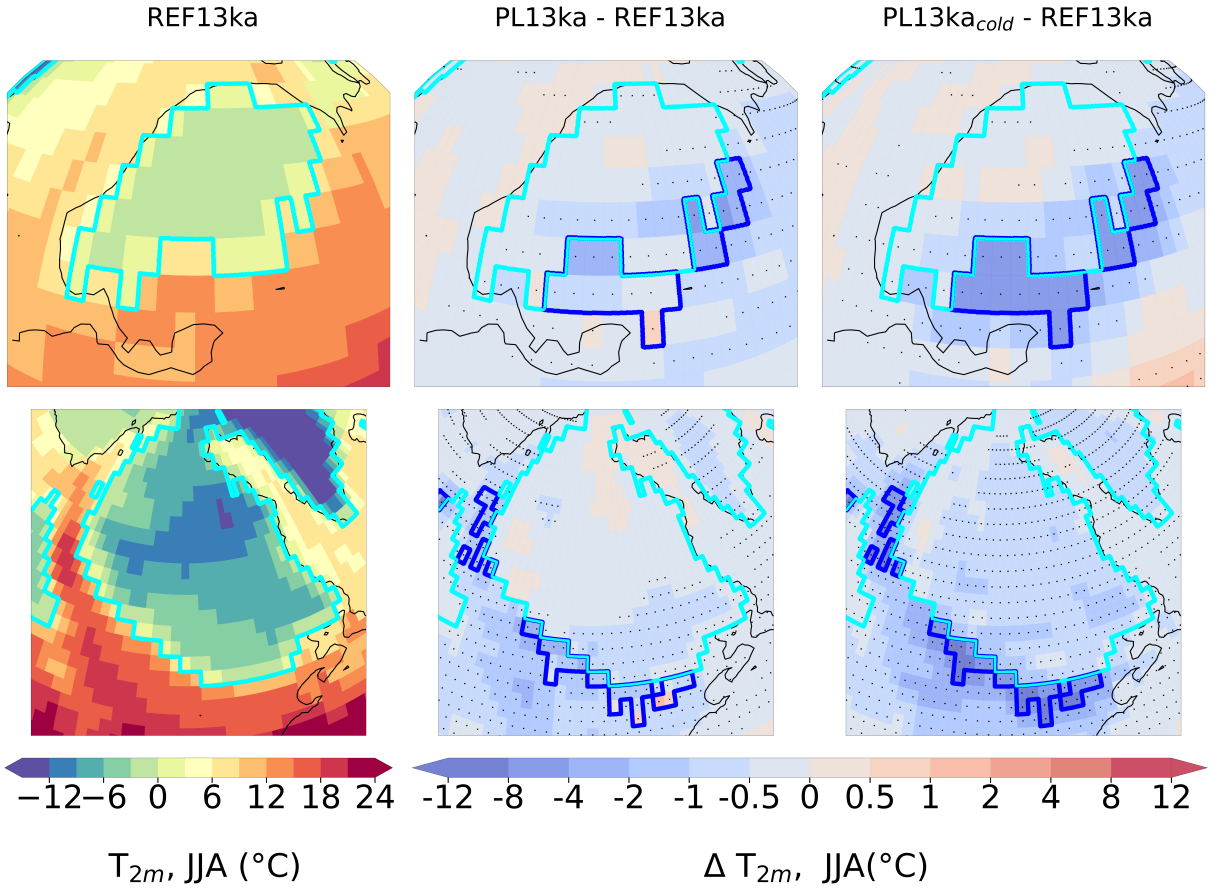


Figure 1. 2m summer temperature for REF13ka (left), REF13ka - PL13ka anomalies (center) and REF13ka - PL13ka$_{cold}$ anomalies (right). Light blue contours indicate ice sheet margins and dark blue lines indicate proglacial lakes. Anomalies which are significant according to a t-test with 95 % confidence level are highlighted by black dots.

approximately 5 % (2 %) in PL13ka$_{cold}$ (PL13ka). Significantly drier climates are found in the direct vicinity of the LIS-PLs and over most parts of the ice sheet, while regions south of the lakes experience enhanced precipitation.

3.2 Surface mass balance

At 13ka the northern hemisphere ice sheets were already strongly reduced with the LIS and FIS covering respectively 8.2 Million km^2 and 1.2 Million km^2 according to the GLAC1D reconstruction. During this period both ice sheets were losing mass at fast rates, which implies that the SMB of the ice sheets must have been too low, possibly even negative to balance the dynamic mass loss through calving. In the following surface mass balance is considered as:

$$SMB = snow + refreezing - melt \quad (1)$$

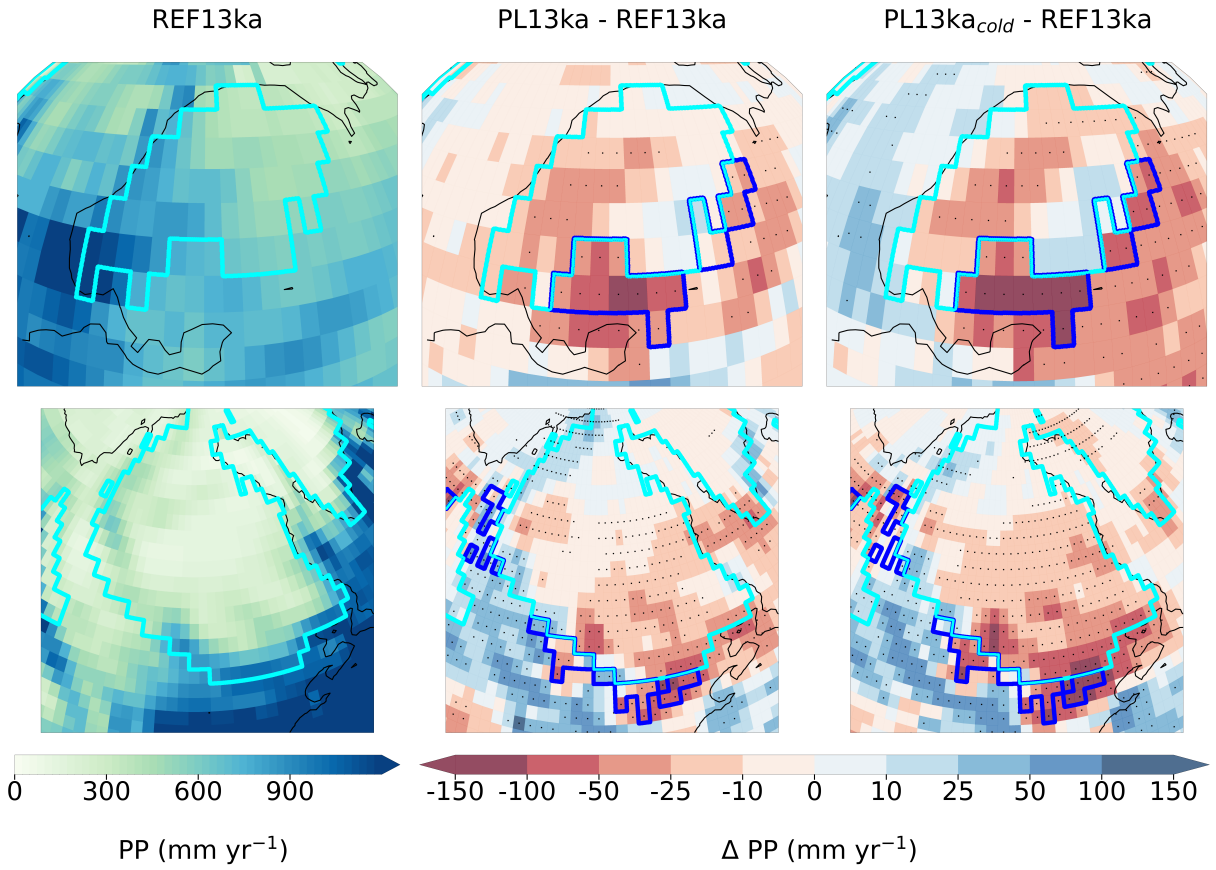


Figure 2. Annual precipitation for REF13ka (left), REF13ka - PL13ka anomalies (center) and REF13ka - PL13ka$_{cold}$ anomalies (right). Light blue contours indicate ice sheet margins and dark blue lines indicate proglacial lakes. Anomalies which are significant according to a t-test with 95 % confidence level are highlighted by black dots.

and runoff as

$$RU = rain + melt - refreezing \tag{2}$$

Table 1 shows our modeled SMB and the components, which define SMB and runoff calculated separately for both considered ice sheets as multi-year means of the annual mean mass changes.

The prescribed geometry of the FIS and LIS indicates that the deglaciation of the two ice sheets is at different stages. The FIS is characterized by a gentle slope and low elevation torwards its continental margins, indicating advanced mass loss, while the LIS has steeper slopes at its margins and the interior is still mostly at heights of more than 1000 m (Fig. S1). In consequence the LIS surface mass balance is positive but small (286 Gt) relative to the spatial dimension of the ice sheet (today's Greenland ice sheet needs to have a SMB of approximately 400 Gt to balance mass loss from calving (Mankoff et al., 2019)) and the total SMB

Table 1. SMB and subcomponents of SMB and runoff from dEBM for both ice sheets in [Gt/year].

	Variable	REF13ka	PL13ka	PL13ka$_{cold}$
FIS	SMB	-754	-335	-204
	snow	650	650	656
	refreeze	187	174	167
	melt	1591	1158	1027
	rain	133	117	109
LIS	SMB	286	778	887
	snow	2744	2709	2659
	refreeze	579	565	557
	melt	3038	2496	2329
	rain	233	189	158

of the FIS is strongly negative due to an extensive ablation zone. Including PLs in experiment PL13ka$_{cold}$ increases the SMB of the FIS and LIS by 550 Gt and 601 Gt respectively and consequently stabilizes both ice sheets (Fig. 3). Primarily the PLs reduce surface melt due to the cooler summer temperatures, by approximately 23 % (18 %) for the LIS and by 36 % (27 %) for the FIS in experiment PL13ka$_{cold}$ (PL13ka). Seasonal analysis (Supplement Table S1 and S2) reveals that in both experiments the onset of the melt season is delayed and weakened, while there is no effect detected in winter. Only in experiment PL13ka does the melt season last well into the autumn due to the capacity of the warm lakes to store and later release heat. The slightly drier climate over the ice sheets is not fully reflected in accordingly reduced snow fall. Snow fall over the FIS is even enhanced, which can be explained with a shift in the snow/rain ratio at lower altitudes caused by the colder climate (Fig. S6 in Supplement). We would like to note that surface melt in dEBM is also sensitive to changes in precipitation during the melt season due to the albedo feedback (Niu et al., 2024): decrease in snow fall may result in lower albedo and higher surface melt, while a decrease in rain will act in the opposite direction. Seasonality in snow, rain and total precipitation are also shown in Fig. S6 in the supplement for both ice sheets.

3.3 Sensitivity of the temperature-melt relation to local climate

Ice-sheet surface mass balance exhibits strong spatial gradients at scales of a few kilometers, so atmospheric fields from global climate models at typical grid scales of the order 100 km are too coarse to resolve key processes in the narrow ablation zones with steep topographic gradients, introducing substantial biases in both regional and integrated SMB estimates (van den Broeke et al., 2017). Consequently available SMB estimates for paleo-ice sheets often draw on statistically downscaled atmospheric forcing (< 20 km) in combination with temperature-index methods to estimate melt (e.g. Yang et al., 2022). These empirical

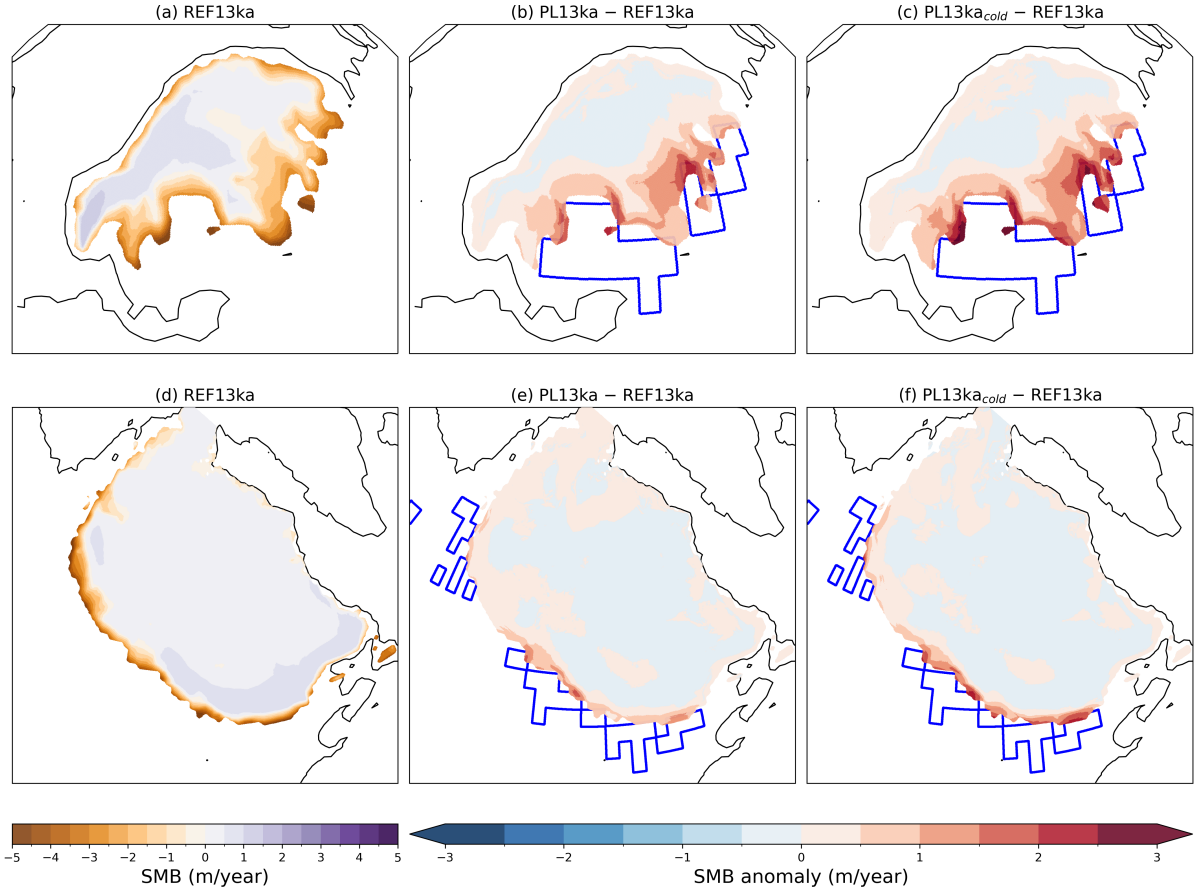


Figure 3. Annual SMB for REF13ka (left) as well as the anomaly between PL13ka and REF13ka (center), and between PL13ka$_{cold}$ and REF13ka (right). The upper row shows the FIS; the lower row shows LIS. Blue lines indicate proglacial lakes.

~~method~~ methods are grounded in the observation that surface melt rates generally increase linearly with positive-degree days, PDDs, where PDD refers to the temporal integral of near-surface temperatures exceeding the melting point (Calov and Greve, 2005). For the present-day climate the PDD approach has demonstrated good skill in deducing surface melt of the Greenland Ice Sheet from near surface air temperatures (Fettweis et al., 2020). However, the surface mass balance does not only depend on temperature and precipitation but radiation considerably influences the temperature - melt relation. It remains unclear whether the same empirical parameters are globally applicable or suitable in different climate periods. To investigate this we assess the sensitivity of the temperature–melt relationship as simulated by the physics-based dEBM to identify potential limitations of empirical methods. The LIS and FIS in our experiments differ in shape, latitudinal position and the influence of adjacent continents and oceans, offering a broader range of climate conditions than the modern Greenland Ice Sheet. Considering both ice sheets we find that for any given PDD value melt rates may vary by a factor of two or more due to variations in incoming shortwave radiation (Fig. 4, left). Experiments PL13ka$_{cold}$ and REF13ka generally exhibit a similar temperature - melt relation

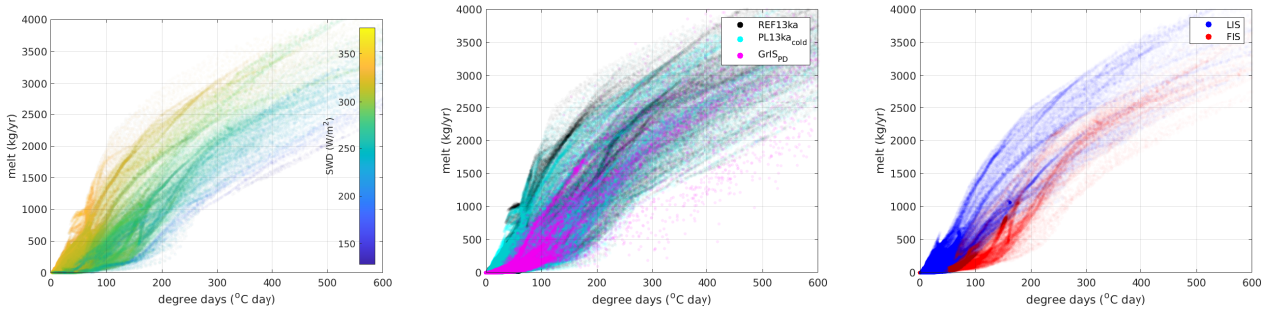


Figure 4. Annual melt versus annual positive degree days. Each circle represents the multi-year mean for an individual ice covered gridpoint. Left: experiment PL13ka$_{cold}$, including LIS, FIS, Cordillearan and Greenland Ice Sheet, colors represent the mean downward shortwave radiation weighted by melt rates. Center: Colors identify experiment REF13ka (black), experiment PL13ka$_{cold}$ (cyan) and the last 30 years of the 20th century in a historical simulation downscaled with dEBM for the present-day Greenland Ice Sheet (magenta, Verjans et al. (2025)). Right: experiment PL13ka$_{cold}$, colors identify the Laurentide (blue) and Fennoscandian Ice Sheet (red).

(Fig. 4, center). However, when compared with dEBM surface melt rates over Greenland from the last 30 years of a historical simulation (Verjans et al., 2025), we find that here melt appears less efficient (similar temperatures will produce less melt) and the parameter space is narrowed as shortwave radiation is generally less intense. Furthermore, the temperature-melt relation differs between the FIS and LIS (Fig. 4, right). Melt is most efficient over parts of the LIS, particularly away from the coast at the southern and western margin of the Laurentide Ice Sheet where diurnal insolation maxima are intensified due to the lower latitude and less cloud cover. These findings underscore that empirical temperature-index methods would require region-specific parameters, and those derived from present-day Greenland observations are unlikely to be accurate for paleo-ice sheets.

4 Discussion

4.1 Surface mass balance response to proglacial lakes under deglacial conditions

Using a physics-based surface energy-mass balance model, this sensitivity study demonstrates that large proglacial lakes can substantially reduce surface ablation of adjacent ice sheets during deglaciation. For both the Laurentide and Fennoscandian ice sheets, total surface melt is reduced by more than 20-35 % when proglacial lakes are present, with approximately one quarter of this reduction attributable to the maintenance of a perennially cold lake surface. In agreement with earlier studies (Hostetler et al., 2000; Krinner et al., 2004), we find that proglacial lakes induce regional summer cooling over adjacent ice sheets, while accumulation over the Laurentide Ice Sheet is slightly reduced (<2 %). This reduction in accumulation weakens the surface mass balance response only marginally, as the decrease in melt dominates. The relative sensitivity of surface melt to the presence of proglacial lakes under deglacial conditions is comparable to that reported for peak glacial conditions (Colleoni et al., 2009) and also ice-dammed lakes developing during the early inception of the Eurasian Ice Sheet Complex

are found to exert a similar effect (Krinner et al., 2004; Peyaud et al., 2007). However, the resulting impact on total surface mass balance differs markedly during deglaciation, because the ratio of ablation to accumulation is substantially higher. In the present experiments, the lowered ice-surface and reduced slope of the southward facing part of the Fennoscandian Ice Sheet (FIS) leads to a widening of the ablation zone while the Laurentide Ice Sheet (LIS) is less advanced and does not yet show advanced downwasting. As a result, total ablation exceeds accumulation by more than a factor of two for the FIS and is likely to become more dominant as deglaciation progresses. This contrasts with conditions during the peak of the penultimate glacial period (around 140ka), when accumulation was the dominant component of the surface mass balance (Colleoni et al., 2009).

4.2 Balance between dynamical ice loss and climatic SMB feedbacks

Proglacial lakes exert a dual influence on ice-sheet evolution through opposing climatic and dynamic feedbacks, potentially decoupling deglacial ice-sheet behavior from global climate forcing. We find that explicitly coupling proglacial lakes to the climate system increases the surface mass balance of neighbouring ice sheets by suppressing summer melt and reducing mass loss by roughly 20–30 %. The simulated absolute increase in surface mass balance of both ice sheets combined corresponds to a sea-level equivalent of more than 30 cm per 100 years, opposing deglacial sea level rise which by comparison was in the order of 1 m per 100 years over the main deglaciation (Lambeck et al., 2014). For the Laurentide Ice Sheet proglacial lakes increase surface mass balance and reduce mass loss by ∼600 Gt per year for the geometry considered here. In a simulation with a fast retreating interactive ice sheet, this negative feedback would become even larger through the melt–elevation feedback under progressive downwasting of the ice sheet. Complementary to this negative feedback, recent modeling studies have studied the positive dynamic feedback, while neglecting the climate response. Proglacial lake-induced ice-sheet instabilities (PLISI) may increase Laurentide Ice Sheet mass loss by more than 3000 Gt per year ~~Quiquet et al. (2021)~~(Quiquet et al., 2021). Our results suggest that the deglaciation of Northern Hemisphere ice sheets may have been modulated by the balance between opposing dynamical and climatic effects. A conceptual picture emerges in which lake-induced instabilities initially promote rapid mass loss and margin retreat, followed by a phase in which sufficiently large proglacial lakes exert a stabilizing climatic influence by cooling the regional atmosphere and reducing ablation. Indeed Austermann et al. (2022) find that between 14.2 and 11.5 ka, retreat rates inferred from geological reconstructions were significantly higher at lake-terminating than at land-terminating margins, whereas this contrast was less pronounced before and after this interval. However, sensitivity studies also reveal that the strength of the dynamic feedback strongly depends on complex processes and poorly constrained basal boundary conditions, including basal friction, ice–lake interactions, glacial isostatic adjustment, and changing lake levels or drainage events (Scherrenberg et al., 2024; Austermann et al., 2022; Hu and Haseloff, 2025)~~, which may be another reason~~. These factors may explain why both ice sheets exhibit a more heterogeneous retreat history in geological reconstructions than in the above simulations with ice-only models or models of intermediate complexity: The southern Laurentide Ice Sheet exhibits highly variable ice-stream configurations and periods of stagnation and readvance ~~(Dyke, 2004; Margold et al., 2018; Dalton et al., 2020; Norris et al., 2024, e.g.)~~ (e.g. Dyke, 2004; Margold et al., 2018; Dalton et al., 2020; Norris et al., 2024) and contrasting retreat patterns of the Fennoscandian Ice Sheet between ~~Bølling~~Bølling–~~Allerød~~ Allerød and Younger Dryas despite a continuous presence of the Baltic Ice Lake (Stroeven et al., 2016).

4.3 Limitations and implications for surface mass balance parameterizations

Several limitations of the present experiments should be noted. The prescribed ice-sheet geometry does not allow for elevation-surface mass balance feedbacks, which may alter the magnitude of the surface mass balance response during ongoing retreat. Furthermore, the hybrid boundary conditions employed here are not intended to reproduce a realistic deglacial trajectory, but rather to isolate the sensitivity of climate and surface mass balance to proglacial lakes under deglacial conditions. Our results further indicate that variations in incoming shortwave radiation substantially modify the relationship between near-surface temperature and melt. This finding highlights limitations of empirical temperature-index approaches when applied across different regions or climate states. Nevertheless, temperature-index methods may yield reliable surface mass balance estimates if temperatures are downscaled to sufficiently high spatial resolution and model parameters are adjusted to account for regional and climatic differences, as e.g. in (Colleoni et al., 2009). These considerations are particularly relevant for large-scale ice-sheet modeling studies that rely on simplified surface mass balance parameterizations.

4.4 Toward fully coupled lake-ice-atmosphere modeling

Fully assessing the complex interplay between proglacial lakes, ice sheets, and the atmosphere during deglaciation ultimately requires transient, fully coupled Earth system simulations that explicitly represent lake-ice, lake-atmosphere, and atmosphere-ice interactions. In recent years, important developments have emerged for all three interfaces, providing a pathway toward such comprehensive modeling frameworks. These include Lake-CC for efficiently representing lake basins and lake-ice interactions (Hinck et al., 2020), ECHAM6 with a proglacial lake extension for representing lake-atmosphere coupling (this study, ECHAM6-PL), and coupled atmosphere-ice approaches that resolve energy and mass exchange at the ice surface (Vizcaino et al., 2010; Krebs-Kanzow et al., 2021; Born et al., 2019).

Integrating these developments into transient simulations offers the potential to quantify the evolving balance between dynamical ice loss and climatically driven surface mass balance feedbacks during glacial terminations.

5 Conclusion

Using a physics-based surface energy-mass balance approach, we show that large proglacial lakes can substantially reduce surface ablation of adjacent ice sheets during deglaciation, decreasing total melt by more than 20-35 % for the Laurentide and Fennoscandian ice sheets under Allerød-like conditions. Approximately one quarter of this reduction arises from the maintenance of a perennially cold lake surface, highlighting the importance of ice-lake thermal interactions. Although proglacial lakes slightly reduce accumulation, this effect is small compared to the reduction in melt, resulting in a net increase in surface mass balance. Because ablation dominates surface mass balance during deglaciation, the climatic impact of proglacial lakes is amplified relative to glacial conditions. Our results indicate that proglacial lakes can partially counteract dynamically driven ice loss and thereby modulate the pace of ice-sheet retreat. Accounting for the influence of proglacial lakes during glacial terminations may therefore improve ice-sheet model projections.

Data availability. The analysis scripts and data used for figures in this study are available at https://zenodo.org/, Gierz et al. (2026)

Author contributions. UKK, LS and GL conceptualized the original ideas presented in this manuscript. LS and PG implemented the lake extension in ECHAM6, GK provided ocean boundary conditions, LN and LS defined the lake configuration with LakeCC. LS carried out atmosphere model experiments and LS and UKK conducted SMB simulations. LS and UKK conducted the analysis of the model results and wrote the initial draft of the manuscript. All authors contributed to the interpretation of results and manuscript preparation.

Competing interests. None of the authors has any competing interests.

Acknowledgements. ~~We are grateful to Kai Himstedt and Sebastian Hinck from DKRZ for ECHAM6 and LakeCC support.~~

6 ~~Supplemental Materials: Proglacial lakes substantially modulate the surface mass balance of deglacial ice sheets~~

5.1 ~~Ice sheet configuration~~

~~Northern hemisphere ice cover at 13 ka according to Tarasov et al. (2012).~~

5.1 ~~Seasonality of Climate and Surface Mass Balance~~

~~Mean summer precipitation (JJA) anomaly with respect to REF13ka for experiment PL13ka$_{cold}$ (a) and PL13ka (b), and difference between experiment PL13ka$_{cold}$ and PL13ka (c). Anomalies which are not significant according to a t-test with 95% confidence level are masked out. Black contours indicate ice sheet margins and cyan lines indicate proglacial lakes. The topography of the ice sheets at 5km resolution which was used for the SMB calculation is depicted as grey contours for 1000, 2000 and 3000m elevation.~~

~~Same as Fig. **??** but for mean winter precipitation anomaly (DJF)~~

~~Same as Fig. **??** but for summer near surface temperatures~~ ~~Same as Fig. **??** but for winter near surface temperatures.~~ ~~Monthly mean total precipitation (solid lines), snow (dash-dotted) and rain (dotted) over the Fennoscandian and Laurentide Ice sheets for the experiments REF13ka (black), PL13ka (red) and PL13ka$_{cold}$ (cyan)~~

~~FIS seasonal contributions to SMB in GT/season.~~ ~~Variable REF13ka PL13ka PL13ka$_{cold}$ SMB 145 151 146 snow 145 151 146 refreeze 0 0 0 melt 0 0 0 rain 0 0 0 SMB 136 145 153 snow 167 151 157 refreeze 28 14 13 melt 58 21 17 rain 5 3 2 SMB -1230 -822 -715 snow 126 133 137 refreeze 146 145 141 melt 1502 1099 992 rain 108 93 90 SMB 195 191 210 snow 213 214 214 refreeze 14 14 13 melt 31 38 17 rain 19 21 17~~

~~LIS seasonal contributions to SMB in GT/season.~~ ~~Variable REF13ka PL13ka PL13ka$_{cold}$ SMB 401 396 400 snow 401 396 400 refreeze 0 0 0 melt 0 0 0 rain 0 0 0 SMB 517 507 507 snow 564 531 529 refreeze 32 20 20 melt 80 44 42 rain 4 1 1 SMB -1366 -880 -807 snow 969 939 914 refreeze 524 519 517 melt 2860 2339 2238 rain 207 158 140 SMB 733 755 787 snow 810 843 816 refreeze 22 25 20 melt 98 113 49 rain 23 30 17~~

5.1 ~~Estimating the mass of ice that needs to melt at the ice-lake interface to maintain cold summer surface temperatures in experiment PL13ka$_{cold}$~~

~~Recent surface temperature observations from present-day proglacial lakes show maximum summer values of 4 to 6 C (Sugiyama et al., 2021; ?) . However, these lakes are not a perfect analogue for the much larger proglacial lakes at the margins of the rapidly retreating ice sheets of the Allerød and their surface temperature is not known. By capping surface temperatures at 4 C in experiment PL13ka$_{cold}$, we have chosen a scenario at the lower end of the likely temperature spectrum. Overriding simulated lake surface temperatures creates a heat sink within the model, which should be interpreted as heat loss from melting ice in the proglacial lakes. Our experiment design does not allow us to quantify the effective heat loss. As a makeshift solution we here apply a simple one-dimensional thermodynamic lake model to estimate the amount of ice that would need to melt in the lake to generate the same surface temperature as in experiment PL13ka$_{cold}$.The lake model is a finite difference model resolving the 1D vertical temperature profile of a lake by discretizing the water column and solving the diffusion equation at equidistant layers. Input for the lake model is taken from atmospheric output of experiments PL13ka and PL13ka$_{cold}$: as forcing we use 2m-temperature, downward longwave radiation, downward shortwave radiation and seaice cover from multi-year monthly means averaged over the proglacial lakes at the southern margins of the North American (south of 55 N, LIS-PLforcing~~UKK acknowledges funding from the Deutsche Forschungsgemeinschaft (DFG, German Research Foundation) under Germany's Excellence Strategy – Cluster of Excellence "The Ocean Floor – Earth's Uncharted Interface" (EXC 2077, Project 390741603), and ~~Fennoscandian Ice Sheets (FIS-PL forcing) and we use corresponding surface temperatures to evaluate and constrain the lake model. At first we use forcings from experiment PL13ka and choose model parameters so that surface temperatures simulated by the lake model agree reasonably well with the surface temperatures from the atmospheric output over the respective lakes (Fig. S7, solid lines). We then use the same model parameters in combination with forcing from experiment PL13ka$_{cold}$, but here every time step we additionally cool the lake surface to the lake surface temperature from PL13ka$_{cold}$ and calculate the corresponding heat flux required for this cooling (Fig. S7, dashed lines). All experiments are initialized with a uniform temperature of 4 C and are equilibrated with yearly repeating forcing over 250 years. The model assumes no horizontal heat transport and neglects advective processes. **Result**: Our model experiments exhibt seasonal temperature variations in the upper 20 m of the water column and constant temperature of 4 C at depth (Fig. S8) . When we apply forcing and additional cooling from experimrent PL13ka$_{cold}$ the respective accumulated heat loss per year is $0.7 \times 10^9\ Wm^{-2}$ for the FIS-PL forcing and $1.2 \times 10^9\ Wm^{-2}$ for the LIS-PL forcing which corresponds to approximately 215 Gt and 360 Gt of melting ice that is required to cool a lake area of 100000 km^2 accordingly.~~

~~Annual lake surface temperature for FIS-PL forcing (upper panel) and LIS-PL forcing (below) from atmosphere model (black) and one-dimensional lake model (red). Solid lines are for forcing from experiment PL13ka and dashed line are for experiment PL13ka$_{cold}$~~from the European Union's Horizon Europe programme through the LiquidIce project (Grant Agreement No. 101184962). This project was also supported by the German Federal Ministry of Education and Research (BMBF) through the PalMod project (grant numbers 01LP1915A and 01LP2303A to G.K.~~Temperature stratification in the upper 40m of the lake model for FIS-PL (left panel) and LIS-PL (right) forcing from experiment PL13ka (upper panel) and for experiment PL13ka$_{cold}$ (below).~~

~~**Model Configuration**~~

~~**Spatial and Temporal Discretization**~~

Vertical Grid: The water column is divided into i=0..49 equidistant layers with a water temperature T_i and thickness `dz` = 4 m. Mixed Layer Depth: A mixed layer depth (`mld` = 12 m) is used to parameterize vertical diffusivity. Time Stepping: The model uses a daily time step (`dt` = 86, 400 s) and simulates 250 years to reach equilibrium.

Physical parameters

Thermal diffusivity:

$$\alpha_i = \begin{cases} 2 \times 10^{-5}\ \mathrm{m}^2/\mathrm{s}, & i\,dz \le \mathrm{mld}, \\ 5 \times 10^{-7}\ \mathrm{m}^2/\mathrm{s}, & i\,dz > \mathrm{mld}. \end{cases}$$

Water properties:

- Density (ρ_w) = 1,000 kg/m^3
- Specific heat capacity (c_{pw}) = 4,186 J/kg·K
- Latent heat of fusion (L_i) = 334,000 J/kg
- Freezing point (Tf) = 273.15 K

Parameters of the surface energy balance: Emissivity of water (ϵ_w) = 0.97 Stefan–Boltzmann constant ($\sigma = 5.67 \times 10^{-8}\ W/m^2/K^4$) Heat transfer coefficient ($h = 30\ W/m^2/°C$ for LIS-PL and $h = 20\ W/m^2/°C$ for FIS-PL forcing)

Calculation of the surface temperature T_0

The model is forced by the surface heat flux (Q_{surface}) which is calculated as:

$$Q_{\text{surface}} = \mathrm{SWD} + \mathrm{LWD} - \mathrm{LWU} + \mathrm{SHF}$$

where: LWU = upward longwave radiation ($\epsilon_w \sigma T_0^4$ 01LP1916B and 01LP2313A to G.L.) SHF = sensible heat flux ($h(T_{\text{air}} - T_0)$) temperature of lake surface (prognostic) T_0 The climate forcing is derived from monthly mean climate output (interpolated to daily resolution) averaged over proglacial lakes of the LIS and FIS from experiment PL13ka or PL13ka$_{cold}$.

- 2-m air temperature, T_{air}
- Incoming shortwave radiation, `SWD`
- Downward longwave radiation, `LWD`
- Sea ice cover, `seaice`
- Surface temperature from atmospheric output, T_{surf}

Each timestep the temperature of ice-free parts of the surface are computed:

$$T_{\text{ice free}} = \max(T_f, T_{\text{surf}} + \frac{Q_{\text{surface}}}{\rho_w c_{pw} \Delta z} \Delta t)$$

and ice covered parts are assumed to be at freezing point.The temperature of the surface layerT_0 is set to

$$T_0 = (1 - \mathrm{seaice}) T_{\text{ice free}} + \mathrm{seaice} T_f$$

Proglacial Cooling Constraint:For proglacial lakes, the surface temperature of ice free parts of the lake is further constrained to not exceed the surface temperature of experiment PL13ka$_{cold}$.The additional energy required to enforce this cooling (dQ)is calculated as:

$$dQ = (T_0 - T_{\text{surf}})(\rho_w c_{pw} \Delta z)$$

Calculation of the temperature profile:

Temperatures in the water column are updated using a finite difference scheme of heat diffusion:

$$\frac{\partial T_i}{\partial t} = \frac{1}{\Delta z}\left[\alpha_{\text{if}} \frac{T_{i+1} - T_i}{\Delta z} - \alpha_{\text{if}} \frac{T_i - T_{i-1}}{\Delta z}\right]$$

where α_{if} is the harmonic mean of diffusivities at layer interfaces. Density and Stratification:Density is calculated as a function of temperature:

$$\rho(T) = 5.5289 \times 10^{-8} T^3 - 8.5016 \times 10^{-6} T^2 + 6.5622 \times 10^{-5} T + 0.99987$$

If the water column becomes unstable (ρ decreases with depth), layers are adiabatically reordered to enforce stable stratification.

Ice Melt Estimation

The total mass of ice melt (dM) required to maintain the cool lake surface temperatures of experiment PL13ka$_{cold}$ is calculated by integrating the additional energy consumption over a lake area ($100,000$ km$^2 = 1 \times 10^{11}$ m^2):

$$dM = \sum(dQ) \times (1 \times 10^{11}\ \text{m}^2)/L_i/(1 \times 10^{12}\ \text{kg/Gt})$$

urlstyleDye, A., Bryant, R., Falcini, F., Mallalieu, J., Dimbleby, M., Beckwith, M., Rippin, D., and Kirchner, N.: Warm proglacial lake temperatures and thermal undercutting enhance rapid retreat of an Arctic glacier, *The Cryosphere*, 19, 4471–4486, https://doi.org/10.5194/tc-19-4471-2025 2025.

. Sugiyama, S., Minowa, M., Fukamachi, Y., Hata, S., Yamamoto, Y., Sauter, T., Schneider, C., and Schaefer, M.: Subglacial discharge controls seasonal variations in the thermal structure of a glacial lake in Patagonia, *Nature Communications*, 12, 6301, https://doi.org/10.1038/s41467-021-2 2021.

. Tarasov, L. , Dyke, A. S., Neal, R. M., and Peltier, W. R.: A data-calibrated distribution of deglacial chronologies for the North American ice complex from glaciological modeling, Earth Planet. Sci. Lett., 315–316, 30–40, https://doi.org/10.1016/j.epsl.2011.09.010, 2012.

6 Supplemental Materials: Proglacial lakes substantially modulate the surface mass balance of deglacial ice sheets

5.1 Ice sheet configuration

Northern hemisphere ice cover at 13 ka according to Tarasov et al. (2012).

5.1 Seasonality of Climate and Surface Mass Balance

Mean summer precipitation (JJA) anomaly with respect to $REF13ka$ for experiment $PL13ka$ (a) and $PL13ka_{warm}$ (b), and difference between experiment $PL13ka$ and $PL13ka_{warm}$ (c). Anomalies which are not significant according to a t-test with 95% confidence level

are masked out. Black contours indicate ice sheet margins and cyan lines indicate proglacial lakes. The topography of the ice sheets at 5km resolution which was used for the SMB calculation is depicted as grey contours for 1000, 2000 and 3000m elevation.

Same as Fig. **??** but for mean winter precipitation anomaly (DJF)

Same as Fig. **??** but for summer near surface temperatures Same as Fig. **??** but for winter near surface temperatures. Monthly mean total precipitation (solid lines), snow (dash-dotted) and rain (dotted) over the Fennoscandian and Laurentide Ice sheets for the experiments $REF13ka$ (black), $PL13ka_{warm}$ (red) and $PL13ka$ (cyan)

FIS seasonal contributions to SMB in GT/season. Variable $REF13ka$ $PL13ka_{warm}$ $PL13ka$ SMB 145 151 146 snow 145 151 146 refreeze 0 0 0 melt 0 0 0 rain 0 0 0 SMB 136 145 153 snow 167 151 157 refreeze 28 14 13 melt 58 21 17 rain 5 3 2 SMB -1230 -822 -715 snow 126 133 137 refreeze 146 145 141 melt 1502 1099 992 rain 108 93 90 SMB 195 191 210 snow 213 214 214 refreeze 14 14 13 melt 31 38 17 rain 19 21 17

LIS seasonal contributions to SMB in GT/season. Variable $REF13ka$ $PL13ka_{warm}$ $PL13ka$ SMB 401 396 400 snow 401 396 400 refreeze 0 0 0 melt 0 0 0 rain 0 0 0 SMB 517 507 507 snow 564 531 529 refreeze 32 20 20 melt 80 44 42 rain 4 1 1 SMB -1366 -880 -807 snow 969 939 914 refreeze 524 519 517 melt 2860 2339 2238 rain 207 158 140 SMB 733 755 787 snow 810 843 816 refreeze 22 25 20 melt 98 113 49 rain 23 30 17

5.1 Estimating the mass of ice that needs to melt at the ice-lake interface to maintain cold summer surface temperatures in experiment $PL13ka$

Recent surface temperature observations from present-day proglacial lakes show maximum summer values of 4 to 6 C (Sugiyama et al., 2021; **?**) . However, these lakes are not a perfect analogue for the much larger proglacial lakes at the margins of the rapidly retreating ice sheets of the Allerød and their surface temperature is not known. By capping surface temperatures at 4 C in experiment $PL13ka$, we have chosen a scenario at the lower end of the likely temperature spectrum. Overriding simulated lake surface temperatures creates a heat sink within the model, which should be interpreted as heat loss from melting ice in the proglacial lakes. Our experiment design does not allow us to quantify the effective heat loss. As a makeshift solution we here apply a simple one-dimensional thermodynamic lake model to estimate the amount of ice that would need to melt in the lake to generate the same surface temperature as in experiment $PL13ka$. The lake model is a finite difference model resolving the 1D vertical temperature profile of a lake by discretizing the water column and solving the diffusion equation at equidistant layers. Input for the lake model is taken from atmospheric output of experiments $PL13ka_{warm}$ and $PL13ka$: as forcing we use 2m-temperature, downward longwave radiation, downward shortwave radiation and seaice cover from multi-year monthly means averaged over the proglacial lakes at the southern margins of the North American (south of 55 N, LIS-PLforcing) , and Fennoscandian Ice Sheets (FIS-PL forcing)and we use corresponding surface temperatures to evaluate and constrain the lake model. At first we use forcings from experiment $PL13ka_{warm}$ and choose model parameters so that surface temperatures simulated by the lake model agree reasonably well with the surface temperatures from the atmospheric output over the respective lakes (Fig. S7, solid lines). We then use the same model parameters in combination with forcing from experiment $PL13ka$, but here every time step we additionally cool the lake surface to the lake surface temperature from $PL13ka$ and calculate the corresponding heat flux required for this cooling (Fig. S7, dashed lines). All experiments are initialized with a uniform temperature of 4 C and are equilibrated with yearly repeating forcing over 250 years. The model assumes no horizontal heat transport and neglects advective processes. **Result**: Our model experiments exhibt seasonal temperature variations in the upper 20 m of the water column and constant temperature of 4 C at depth (Fig. S8) . When we apply forcing and additional cooling from experimrent $PL13ka$ the respective accumulated heat loss per year is $0.7 \times 10^9\ Wm^{-2}$ for G.L. acknowledges funding from the FIS-PL

forcing and $1.2 \times 10^9\ Wm^{-2}$ for the LIS-PL forcing which corresponds to approximately 215 Gt and 360 Gt of melting ice that is required to cool a lake area of 100000 km^2 accordingly.

Annual lake surface temperature for FIS-PL forcing (lupper panel) and LIS-PL forcing (below) from atmosphere model (black) and one-dimensional lake model (red). Solid lines are for forcing from experiment $PL13ka_{warm}$ and dashed line are for experiment $PL13ka$. Temperature stratification in the upper 40m of the lake model for FIS-PL (left panel) and LIS-PL (right) forcing from experiment $PL13ka_{warm}$ (upper panel) and for experiment $PL13ka$ (below).

Model Configuration

Spatial and Temporal Discretization

- Vertical Grid: The water column is divided into i=0..49 equidistant layers with a water temperature T_i and thickness `dz` = 4 m.
- Mixed Layer Depth: A mixed layer depth (`mld` = 12 m) is used to parameterize vertical diffusivity.
- Time Stepping: The model uses a daily time step (`dt` = 86,400 s) and simulates 250 years to reach equilibrium.

Physical parameters

Thermal diffusivity:

$$\alpha_i = \begin{cases} 2 \times 10^{-5}\ \mathrm{m}^2/\mathrm{s}, & i\,dz \leq \mathrm{mld}, \\ 5 \times 10^{-7}\ \mathrm{m}^2/\mathrm{s}, & i\,dz > \mathrm{mld}. \end{cases}$$

Water properties:

- Density (ρ_w) = 1, 000 kg/m^3
- Specific heat capacity (c_{pw}) = 4,186 J/kg·K
- Latent heat of fusion (L_i) = 334,000 J/kg
- Freezing point (Tf) = 273.15 K

Parameters of the surface energy balance: Emissivity of water (ϵ_w) = 0.97 Stefan–Boltzmann constant ($\sigma = 5.67 \times 10^{-8}\ W/m^2/K^4$) Heat transfer coefficient ($h = 30\ W/m^2/°C$ for LIS-PL and $h = 20\ W/m^2/°C$ European Union through the European Research Council (ERC) grant “i2B” (Grant Agreement No. 101118519). Open-access publication was funded and organized by Projekt DEAL. We thank the Max Planck Institute for Meteorology in Hamburg and our colleagues at the Alfred Wegener Institute (AWI) for FIS-PL forcing)

Calculation of the surface temperature T_0

The model is forced by the surface heat flux (Q_{surface}) which is calculated as:

$$Q_{\text{surface}} = \mathrm{SWD} + \mathrm{LWD} - \mathrm{LWU} + \mathrm{SHF}$$

where:

- LWU = upward longwave radiation ($\epsilon_w \sigma T_0^4$)

- SHF = sensible heat flux ($h(T_{\text{air}} - T_0)$)
- temperature of lake surface (prognostic) T_0

The climate forcing is derived from monthly mean climate output (interpolated to daily resolution) averaged over proglacial lakes of the LIS and FIS from experiment $PL13ka_{warm}$ or $PL13ka_{warm}$.

- 2-m air temperature, T_{air}
- Incoming shortwave radiation, `SWD`
- Downward longwave radiation, `LWD`
- Sea ice cover, `seaice`
- Surface temperature from atmospheric output, T_{surf}

Each timestep the temperature of ice-free parts of the surface are computed:

$$T_{\text{ice free}} = \max(T_f, T_{\text{surf}} + \frac{Q_{\text{surface}}}{\rho_w c_{pw} \Delta z} \Delta t)$$

and ice covered parts are assumed to be at freezing point. The temperature of the surface layerT_0 is set to

$$T_0 = (1 - \text{seaice}) T_{\text{ice free}} + \text{seaice} T_f$$

Proglacial Cooling Constraint:For proglacial lakes, the surface temperature of ice free parts of the lake is further constrained to not exceed the surface temperature of experiment PL13ka. The additional energy required to enforce this cooling (dQ) is calculated as:

$$dQ = (T_0 - T_{\text{surf}})(\rho_w c_{pw} \Delta z)$$

Calculation of the temperature profile:

Temperatures in the water column are updated using a finite difference scheme of heat diffusion:

$$\frac{\partial T_i}{\partial t} = \frac{1}{\Delta z} \left[\alpha_{\text{if}} \frac{T_{i+1} - T_i}{\Delta z} - \alpha_{\text{if}} \frac{T_i - T_{i-1}}{\Delta z} \right]$$

where α_{if} is the harmonic mean of diffusivities at layer interfaces.Density and Stratification:Density is calculated as a function of temperature:

$$\rho(T) = 5.5289 \times 10^{-8} T^3 - 8.5016 \times 10^{-6} T^2 + 6.5622 \times 10^{-5} T + 0.99987$$

If the water column becomes unstable (ρ decreases with depth), layers are adiabatically reordered to enforce stable stratification.

Ice Melt Estimation

The total mass of ice melt (dM) required to maintain the cool lake surface temperatures of experiment PL13ka is calculated by integrating the additional energy consumption over a lake area ($100,000\ \text{km}^2 = 1 \times 10^{11}\ \text{m}^2$):

$$dM = \sum (dQ) \times (1 \times 10^{11}\ \text{m}^2) / L_i / (1 \times 10^{12}\ \text{kg/Gt})$$

urlstyleDye, A. , Bryant, R., Falcini, F., Mallalieu, J., Dimbleby, M., Beckwith, M., Rippin, D., and Kirchner, N.: Warm proglacial lake temperatures and thermal undercutting enhance rapid retreat of an Arctic glacier, *The Cryosphere*, 19, 4471–4486, https://doi.org/10.5194/tc-19-4471-2025 2025.

. Sugiyama, S., Minowa, M., Fukamachi, Y., Hata, S., Yamamoto, Y., Sauter, T., Schneider, C., and Schaefer, M.: Subglacial discharge controls seasonal variations in the thermal structure of a glacial lake in Patagonia, *Nature Communications*, 12, 6301, https://doi. org/10.1038/s41467-021-2 2021.

. Tarasov, L., Dyke, A. S., Neal, R. M., and Peltier, W. R.: A data-calibrated distribution of deglacial chronologies for the North American ice complex from glaciological modeling, Earth Planet. Sci. Lett., 315making the ECHAM6-JSBACH and FESOM2 models available. We are grateful to Kai Himstedt and Sebastian Hinck (Deutsches Klimarechenzentrum, DKRZ) for their support with ECHAM6 and LakeCC. We gratefully acknowledge the computational resources and technical support provided by the AWI computing center in Bremerhaven and the DKRZ in Hamburg, Germany. This work contributes to the Helmholtz research program "Changing Earth –316, 30–40, https://doi.org/10.1016/j.epsl.2011. 2012.Sustaining our Future" and the Helmholtz Climate Initiative "REKLIM". We thank the anonymous reviewers for their thorough reviews and constructive feedback, which helped improve the quality of this manuscript.

References

Andersen, B. and Borns, H.: The Ice Age world: an introduction to Quaternary history and research with emphasis on North America and northern Europe during the last 2.5 million years, 551.33 AND, 1994.

Austermann, J., Wickert, A. D., Pico, T., Kingslake, J., Callaghan, K. L., and Creel, R. C.: Glacial Isostatic Adjustment Shapes Proglacial Lakes Over Glacial Cycles, Geophysical Research Letters, 49, 2022.

Berger, A.: Long-term variations of daily insolation and Quaternary climatic changes, Journal of the Atmospheric Sciences, 35, 2362–2367, 1978.

Born, A., Imhof, M., and Stocker, T.: An efficient surface energy-mass balance model for snow and ice, Cryosphere, 13, 1529–1546, 2019.

Calov, R. and Greve, R.: A semi-analytical solution for the positive degree-day model with stochastic temperature variations, Journal of Glaciology, 51, 173–188, 2005.

Carrivick, J. and Tweed, F.: Proglacial lakes: character, behaviour and geological importance, Quaternary Science Reviews, 78, 34–52, 2013.

Colleoni, F., Krinner, G., Jakobsson, M., Peyaud, V., and Ritz, C.: Influence of regional parameters on the surface mass balance of the Eurasian ice sheet during the peak Saalian (140 kya), Global and Planetary Change, 68, 132–148, 2009.

Dalton, A. S., Margold, M., Stokes, C. R., Tarasov, L., Dyke, A. S., Adams, R. S., Allard, S., Arends, H. E., Atkinson, N., Attig, J. W., Barnett, P. J., Barnett, R. L., Batterson, M., Bernatchez, P., Borns, Jr., H. W., Breckenridge, A., Briner, J. P., Brouard, E., Campbell, J. E., Carlson, Anders, E., Clague, J. J., Curry, B. B., Daigneault, R.-A., Dube-Loubert, H., Easterbrook, D. J., Franzi, D. A., Friedrich, H. G., Funder, S., Gauthier, M. S., Gowan, A. S., Harris, K. L., Hetu, B., Hooyer, T. S., Jennings, C. E., Johnson, M. D., Kehew, A. E., Kelley, S. E., Kerr, D., King, E. L., Kjeldsen, K. K., Knaeble, A. R., Lajeunesse, P., Lakeman, T. R., Lamothe, M., Larson, P., Lavoie, M., Loope, H. M., Lowell, V, T., Lusardi, B. A., Manz, L., McMartin, I., Nixon, F. C., Occhietti, S., Parkhill, M. A., Piper, D. J. W., Pronk, A. G., Richard, P. J. H., Ridge, J. C., Ross, M., Roy, M., Seaman, A., Shaw, J., Stea, R. R., Teller, J. T., Thompson, W. B., Thorleifson, L. H., Utting, D. J., Veillette, J. J., Ward, B. C., Weddle, T. K., and Wright, Jr., H. E.: An updated radiocarbon-based ice margin chronology for the last deglaciation of the North American Ice Sheet Complex, Quaternary Science Reviews, 234, 2020.

Demidov, I. N., Houmark-Nielsen, M., Kjaer, K. H., and Larsen, E.: The last Scandinavian Ice Sheet in northwestern Russia: ice flow patterns and decay dynamics, Boreas, 35, 425–443, 2006.

Dyke, A. S.: An outline of North American deglaciation with emphasis on central and northern Canada, in: Quaternary Glaciations-Extent and Chronology, edited by Ehlers, J. and Gibbard, P., vol. 2 of *Developments in Quaternary Sciences*, pp. 373–424, Elsevier, 2004.

Fettweis, X., Hofer, S., Krebs-Kanzow, U., Amory, C., Aoki, T., Berends, C. J., Born, A., Box, J. E., Delhasse, A., Fujita, K., Gierz, P., Goelzer, H., Hanna, E., Hashimoto, A., Huybrechts, P., Kapsch, M.-L., King, M. D., Kittel, C., Lang, C., Langen, P. L., Lenaerts, J. T. M., Liston, G. E., Lohmann, G., Mernild, S. H., Mikolajewicz, U., Modali, K., Mottram, R. H., Niwano, M., Noël, B., Ryan, J. C., Smith, A., Streffing, J., Tedesco, M., van de Berg, W. J., van den Broeke, M., van de Wal, R. S. W., van Kampenhout, L., Wilton, D., Wouters, B., Ziemen, F., and Zolles, T.: GrSMBMIP: intercomparison of the modelled 1980–2012 surface mass balance over the Greenland Ice Sheet, The Cryosphere, 14, 3935–3958, 2020.

Fisher, T. G.: Megaflooding associated with glacial Lake Agassiz, Earth-Science Reviews, 201, 102 974, 2020.

Gierz, P., Sijbrandij, L., and Krebs-Kanzow, U.: Proglacial lakes substantially modulate the surface mass balance of retreating ice sheets: Data, https://doi.org/10.5281/zenodo.18545093, 2026.

Giorgetta, M., Roeckner, E., Mauritsen, T., Bader, J., Crueger, T., Esch, M., Rast, S., Kornblueh, L., Schmidt, H., Kinne, S., et al.: The atmospheric general circulation model ECHAM6-model description, Max-Planck-Institut für Meteorologie, 2013.

Hinck, S., Gowan, E. J., and Lohmann, G.: LakeCC: a tool for efficiently identifying lake basins with application to palaeogeographic reconstructions of North America, Journal of Quaternary Science, 35, 422–432, 2020.

Hinck, S., Gowan, E. J., Zhang, X., and Lohmann, G.: PISM-LakeCC: Implementing an adaptive proglacial lake boundary in an ice sheet model, The Cryosphere, 16, 941–965, 2022.

Hostetler, S., Bartlein, P., Clark, P., Small, E., and Solomon, A.: Simulated influences of Lake Agassiz on the climate of central North America 11,000 years ago, Nature, 405, 334–337, 2000.

Hu, K. and Haseloff, M.: Proglacial Lake Drainage Events Drive Fast Grounding Line Advance in a Warming Climate, Geophysical Research Letters, 52, 2025.

Köhler, P., Nehrbass-Ahles, C., Schmitt, J., Stocker, T., and Fischer, H.: A 156 kyr smoothed history of the atmospheric greenhouse gases CO 2, CH 4, and N 2 O and their radiative forcing, Earth System Science Data, 9, 363—387, 2017.

Krebs-Kanzow, U., Gierz, P., and Lohmann, G.: Brief communication: An ice surface melt scheme including the diurnal cycle of solar radiation, The Cryosphere, 12, 3923–3930, 2018.

Krebs-Kanzow, U., Gierz, P., Rodehacke, C. B., Xu, S., Yang, H., and Lohmann, G.: The diurnal Energy Balance Model (dEBM): a convenient surface mass balance solution for ice sheets in Earth system modeling, The Cryosphere, 15, 2295–2313, 2021.

Krinner, G., Mangerud, J., Jakobsson, M., Crucifix, M., Ritz, C., and Svendsen, J.: Enhanced ice sheet growth in Eurasia owing to adjacent ice-dammed lakes, Nature, 427, 429—432, 2004.

Lambeck, K., Rouby, H., Purcell, A., Sun, Y., and Sambridge, M.: Sea level and global ice volumes from the Last Glacial Maximum to the Holocene, Proceedings of the National Academy of Sciences, 111, 15 296–15 303, https://doi.org/10.1073/pnas.1411762111, 2014.

Mangerud, J., Jakobsson, M., Alexanderson, H., Astakhov, V., Clarke, G. K., Henriksen, M., Hjort, C., Krinner, G., Lunkka, J.-P., Möller, P., Murray, A., Nikolskaya, O., Saarnisto, M., and Svendsen, J. I.: Ice-dammed lakes and rerouting of the drainage of northern Eurasia during the Last Glaciation, Quaternary Science Reviews, 23, 1313–1332, 2004.

Mankoff, K. D., Colgan, W., Solgaard, A., Karlsson, N. B., Ahlstrom, A. P., van As, D., Box, J. E., Khan, S. A., Kjeldsen, K. K., Mouginot, J., and Fausto, R. S.: Greenland Ice Sheet solid ice discharge from 1986 through 2017, Earth System Science Data, 11, 769–786, 2019.

Margold, M., Stokes, C. R., and Clark, C. D.: Reconciling records of ice streaming and ice margin retreat to produce a palaeogeographic reconstruction of the deglaciation of the Laurentide Ice Sheet, Quaternary Science Reviews, 189, 1–30, https://doi.org/10.1016/j.quascirev.2018.03.013, 2018.

Niu, L., Knorr, G., Krebs-Kanzow, U., Gierz, P., and Lohmann, G.: Rapid Laurentide Ice Sheet growth preceding the Last Glacial Maximum due to summer snowfall, Nature Geoscience, 17, 440–449, 2024.

Norris, S. L., Margold, M., Evans, D. J. A., Atkinson, N., and Froese, D. G.: Dynamical response of the southwestern Laurentide Ice Sheet to rapid Bølling–Allerød warming, The Cryosphere, 18, 1533–1559, https://doi.org/10.5194/tc-18-1533-2024, 2024.

Patton, H., Hubbard, A., Andreassen, K., Auriac, A., Whitehouse, P. L., Stroeven, A. P., Shackleton, C., Winsborrow, M., Heyman, J., and Hall, A. M.: Deglaciation of the Eurasian ice sheet complex, Quaternary Science Reviews, 169, 148–172, https://doi.org/10.1016/j.quascirev.2017.05.019, 2017.

Peyaud, V., Ritz, C., and Krinner, G.: Modelling the Early Weichselian Eurasian Ice Sheets: role of ice shelves and influence of ice-dammed lakes, Climate of the Past, 3, 2007.

Quiquet, A., Dumas, C., Paillard, D., Ramstein, G., Ritz, C., and Roche, D. M.: Deglacial Ice Sheet Instabilities Induced by Proglacial Lakes, Geophysical Research Letters, 48, 2021.

Reick, C., Raddatz, T., Brovkin, V., and Gayler, V.: Representation of natural and anthropogenic land cover change in MPI-ESM, Journal of Advances in Modeling Earth Systems, 5, 459—482, 2013.

Scherrenberg, M. D. W., Berends, C. J., and van de Wal, R. S. W.: Late Pleistocene glacial terminations accelerated by proglacial lakes, Climate of the Past, 20, 1761—1784, 2024.

Schoof, C.: Ice sheet grounding line dynamics: Steady states, stability, and hysteresis, Journal of Geophysical Research-Earth Surface, 112, 2007.

Sidorenko, D., Goessling, H. F., Koldunov, N. V., Scholz, P., Danilov, S., Barbi, D., Cabos, W., Gurses, O., Harig, S., Hinrichs, C., Juricke, S., Lohmann, G., Losch, M., Mu, L., Rackow, T., Rakowsky, N., Sein, D., Semmler, T., Shi, X., Stepanek, C., Streffing, J., Wang, Q., Wekerle, C., Yang, H., and Jung, T.: Evaluation of FESOM2.0 Coupled to ECHAM6.3: Preindustrial and HighResMIP Simulations, Journal of Advances in Modeling Earth Systems, 11, 3794–3815, 2019.

Sijbrandij, L.: The influence of proglacial lakes on climate and surface mass balance of retreating ice sheets: A study of the North American and Scandinavian ice sheets at 13 ka BP, Master's thesis, Alfred Wegener Institute, 2022.

Stevens, B., Giorgetta, M., Esch, M., Mauritsen, T., Crueger, T., Rast, S., Salzmann, M., Schmidt, H., Bader, J., Block, K., Brokopf, R., Fast, I., Kinne, S., Kornblueh, L., Lohmann, U., Pincus, R., Reichler, T., and Roeckner, E.: Atmospheric component of the MPI-M Earth System Model: ECHAM6, Journal of Advances in Modeling Earth Systems, 5, 146–172, 2013.

Stokes, C. and Clark, C.: Evolution of late glacial ice-marginal lakes on the northwestern Canadian Shield and their influence on the location of the Dubawnt Lake palaeo-ice stream, Palaeogeography Palaeoclimatology Palaeoecology, 215, 155–171, 2004.

Stroeven, A. P., Hattestrand, C., Kleman, J., Heyman, J., Fabel, D., Fredin, O., Goodfellow, B. W., Harbor, J. M., Jansen, J. D., Olsen, L., Caffee, M. W., Fink, D., Lundqvist, J., Rosqvist, G. C., Stromberg, B., and Jansson, K. N.: Deglaciation of Fennoscandia, Quarternary Science Reviews, 147, 91–121, 2016.

Tarasov, L., Dyke, A. S., Neal, R. M., and Peltier, W. R.: A data-calibrated distribution of deglacial chronologies for the North American ice complex from glaciological modeling, Earth and Planetary Science Letters, 315, 30—40, 2012.

Teller, J., Leverington, D., and Mann, J.: Freshwater outbursts to the oceans from glacial Lake Agassiz and their role in climate change during the last deglaciation, Quaternary Science Reviews, 21, 879—887, 2002.

Truffer, M. and Motyka, R. J.: Where glaciers meet water: Subaqueous melt and its relevance to glaciers in various settings, Reviews of Geophysics, 54, 220–239, 2016.

van den Broeke, M., Box, J., Fettweis, X., et al.: Greenland Ice Sheet Surface Mass Loss: Recent Developments in Observation and Modeling, Current Climate Change Reports, 3, 345–356, https://doi.org/10.1007/s40641-017-0084-8, 2017.

Verjans, V., Robel, A. A., Ultee, L., Seroussi, H., Thompson, A. F., Ackerman, L., Choi, Y., and Krebs-Kanzow, U.: The Greenland Ice Sheet Large Ensemble (GrISLENS): Simulating the future of Greenland under climate variability, EGUsphere, 2025, 1–47, 2025.

Vincent, C., Auclair, S., and Le Meur, E.: Outburst flood hazard for glacier-dammed Lac de Rochemelon, France, Journal of Glaciology, 56, 91—100, 2010.

Vizcaino, M., Mikolajewicz, U., Jungclaus, J., and Schurgers, G.: Climate modification by future ice sheet changes and consequences for ice sheet mass balance, Climate Dynamics, 34, 301–324, 2010.

Weertman, J.: Stability of the Junction of an Ice Sheet and an Ice Shelf, Journal of Glaciology, 13, 3–11, 1974.

Yang, H., Krebs-Kanzow, U., Kleiner, T., Sidorenko, D., Rodehacke, C. B., Shi, X., Gierz, P., Niu, L., Gowan, E. J., Hinck, S., Liu, X., Stap, L. B., and Lohmann, G.: Impact of paleoclimate on present and future evolution of the Greenland Ice Sheet, PLOS ONE, 17, 1–2, https://doi.org/10.1371/journal.pone.0259816, 2022.